International Journal of Nanotechnology and Application (IJNA)
ISSN (P): 2277-4777; ISSN (E): 2278-9391
Vol. 8, Issue 1, Jun 2018, 1-14

VISIBLE LIGHT ASSISTED PHOTOCATALYTIC ACTIVITY OF Co-DOPED ZnO, In-DOPED ZnO AND (Co, In) CO- DOPED ZnO NANOPARTICLES

P. MALATHY [1] & S. SELVARAJAN[2]

[1]*P. G. & Research Department of Chemistry, Nadar Mahajana Sangam S. Vellaichamy Nadar College, Madurai, Tamil Nadu, India*

[2]*P. G. & Research Department of Chemistry, Thiagarajar College, Madurai, Tamil Nadu, India*

ABSTRACT

Zinc Oxide (ZnO), Cobalt (Co), Indium (In) individually doped and co-doped (Co-In) ZnO nanoparticles were synthesized by the co-precipitation method. UV-visible diffuse reflectance spectroscopy (UV-vis-DRS), X-ray diffraction (XRD), scanning electron microscopy (SEM), transmission electron spectroscopy (TEM), energy dispersive X-ray spectroscopy (EDX), Brunauer-Emmett-Teller (B. E. T) surface area analysis and photoluminescence spectra (PL) were used to characterize the nanoparticles. The as-prepared Co-In-ZnO nanoparticles have an extended light absorption range compared with pure ZnO. The incorporation of Co and Into ZnO produces a decrease in the optical band gap compared to the ZnO and showed highly efficient photocatalytic activity to degrade 94% of methylene blue (MB) dye under visible light irradiation. The enhancement of photocatalytic activity is due to the fact that the modification of ZnO with Co and In can increase the separation efficiency of photogenerated electrons and holes in ZnO. The optimum values of different reaction parameters like theeffect of pH, initial dye concentration and catalyst dosage on the photodegradation of MB were obtained by varying pH (5-12), initial dye concentration (8-12μM) and catalyst dosage (0.25-1.0g/L). Furthermore, the antimicrobial activity and the reusability of Co-In-ZnO was tested. Furthermore, the antimicrobial activity and the reusability of Co-In-ZnO was tested.

KEYWORDS: Photocatalysis, Doping, Visible Light, Co-In-ZnO & Methylene Blue

Received: Feb 20, 2018**; Accepted:** Mar 12, 2018**; Published:** Mar 20, 2018**; Paper Id.:** IJNAJUN20181

Original Article

INTRODUCTION

For the past few decades, with rapidly developing technology, ever increasing population and urbanization, we have been witnessing an alarming rise in the pollution of water all over the globe. Large amounts of colored wastewater are discharged into the natural bodies, releasing toxic and potentially carcinogenic substances, can cause serious harm to the aquatic life [1-3]. ZnO is a low- cost alternative photocatalyst for the photodegradation of several dyes owing to its high photosensitivity and thermal stability [4-10]. In order to improve the photo -response of ZnO doping or surface modification with transition, metal cations have been considered as a possible way to shift the optical absorption towards the visible region [11-15]. The incorporation of Copromoted the charge separation and enhances the high visible light photocatalytic activity [16]. Doping with group III elements such as Al, Ga,and In can significantly enhance the optical properties [17]. Moreover, the simultaneous doping of two kinds of an atom into ZnO has attracted considerable interest. Nano-crystalline catalyst Co-$BiVO_4$ [18] showed a high photocatalytic activity under visible light. M-$BiVO_4$ (M=Ag, Co, and Ni) [19] exhibited a high photocatalytic activity for the degradation of MB and 2,4-dichloro phenol under visible light. The improvement of the photocatalytic activity was

ascribed to the incorporation of Co into the crystal of $BiVO_4$. Nano-crystalline Ag/In_2O_3-TiO_2 [20] showed the enhanced photocatalytic activity for the degradation of Rh-B and methyl ter-butyl ether in the liquid phase under UV light and narrowing the band gap due to the change in the band position caused by the contribution of In.

ZnO nanoparticles modified by co-doping with a transition metal ion and group III elements were not synthesized and their photocatalytic activity was not reported so far. In this study, Co and in co-doped ZnO nanoparticles were prepared by co-precipitation method and its photocatalytic activity were estimated by using MB. MB is a potent cationic dye, most commonly used dye in a paper, textile, cosmetic and pharmaceutical industries [21]. The molecular structure of MB is shown in Figure 1. The effect of various parameters such as pH, an initial concentration of the dye and catalyst dosage has been examined and the results obtained were discussed. Moreover, the antimicrobial activity of Co-In-ZnO nanoparticles has also been investigated.

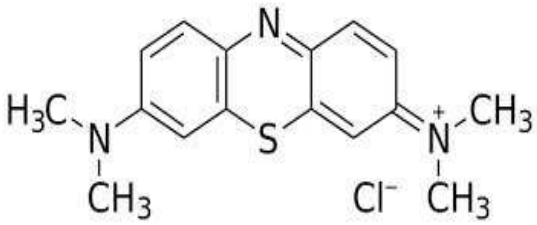

Figure 1: Structure of MB

EXPERIMENTAL

Materials

All the chemicals employed were of analytical grade and applied without further purification. Double distilled water was used throughout the photodegradation experiments.

Synthesis of Co-In-ZnO

A simple co-precipitation method is used to prepare pure ZnO nanoparticles by using ZnSO4.7H2O and NH3 as precursors. CoSO4.7H2O and $In_2(SO_4)_3$ were employed to synthesize co-doped Co-In-ZnO nanoparticles. The Co-In-ZnO was prepared by the following procedure (the molar ratio of Zn: Co: In is fixed in 1: 0.01: 0.01). Initially, 0.25M zinc sulfate solution was taken. For the Co and In dopants, a definite amount of cobalt sulfate and indium sulfate were slowly added individually and combinedly under continuous stirring for 10 min. Then, aqueous ammonia was added drop wise into the above solution with constant stirring until the completion of precipitation. The mixture was stirred at room temperature for 2h. After that, the precipitate was filtered and repeatedly washed with double distilled water to remove impurities. The nanoparticles were obtained after drying at 1100C for 2h followed by calcination at 350ºC for 3h.

Characterization

The crystallite size of the catalyst was examined by X-ray diffractometer (XPERT PRO) with Cu Kα radiation. The optical property was determined by UV diffuse reflectance spectroscopy (JASCO V-550) with PMT detector. Photoluminescence was recorded on the fluorescence spectrometer (Perkin-Elmer LS 55). The surface morphology was characterized by SEM (JSM 6701F---6701) in both secondary and backscattered electron modes. The metal composition was investigated by an energy dispersive X-ray spectroscopy attached to the SEM. The surface morphology was also analyzed by transmission electron microscopy (TEM -TECNAI G2 model). The B. E. The T surface area was measured

through a volumetric adsorption analyzer (MICROMERITICS, ASAP 2020) and the average pore diameters were derived from the N2 adsorption-desorption isotherms by the Barrett-Joyner-Halenda (BJH) method. The photocatalytic experiments were performed in an immersion type photoreactor (HIPR-p-8 /125 /250 /400) and the pH was adjusted using a pH meter (EUTECH).

Photocatalytic Experiment

The photocatalytic experiments were carried out in an immersion type photoreactor. The experimental procedure for photodegradation of MB was similar to our previous report [22]. 200 ml of aqueous solution with 10 μmconcentrations of MB was taken in a cylindrical glass vessel, in which air was bubbling continuously from the bottom of the reactor. Then, the pH of the solution was adjusted using 0.1 N H_2SO_4/ 0.1 N NaOH and required an amount of photocatalyst 0.5g/L was added to the vessel. Before irradiation, the reaction mixture was stirred in the dark for 30 min to achieve the adsorption-desorption equilibrium between the catalyst and dye molecules. A 150 W tungsten lamp was used as the visible light irradiation source. During the course of light irradiation, 5 ml aliquots were withdrawn at a regular time interval of 30 min. Then, the samples were centrifuged and filtered through a Millipore filter to remove the photocatalyst. The filtrate was analyzed by UV–visible spectrophotometer at λ_{max}=664 nm to evaluate the residual MB concentration. Photodegradation (%) = C_0-C/ C_0 X 100 where, C_0 is the concentration of MB before irradiation (t=0) and C is the concentration of MB after a certain irradiation time.

Measurement of Antimicrobial Activity

The antimicrobial activity of the prepared nanoparticles was performed by disc diffusion method using Muller Hinton agar [23]. Two bacterial strains [Staphylococcus aureus and Escherichia coli] and one fungal strain [Candida albicans] were used to study the antimicrobial property. The samples (ZnO, Co-ZnO, In-ZnO and Co-In-ZnO) are dissolved in dimethyl sulfoxide (DMSO) and their concentrations are fixed at 200 μg/ml. (Minimum inhibitory concentration) Amikacin and Ketoconazole were used as a reference drug for antibacterial and antifungal activity respectively. A lawn of test organism was made on the agar plate using a sterile cotton swab and then the antimicrobial discs (Whatman No. 1. Filter disc with samples at 200μg/ml) were placed on the agar plate. The zone of inhibition was measured after an incubation (37ºC) period of 24 h of the cultured agar plates.

RESULTS AND DISCUSSIONS

XRD

The XRD patterns of ZnO, Co-ZnO, In-ZnO and Co-In-ZnO are shown in Figure 2. The diffraction peaks of all samples are quite matching with the hexagonal wurtzite ZnO data (JCPDS NO: 36-1451) and results are depicted in table 1. There is no diffraction peak of impurity phases were detected, confirming the high purity of the synthesized nanoparticles. Co and In are not detected by XRD in the Co-In-ZnO nanoparticles, implying the small amount of Co and In that are highly dispersed on the surface of ZnO. Thus, the ZnO structure is not modified by the addition of Co and In. The crystallite sizes of the synthesized nanoparticles were estimated by Scherrer equation. $D=0.89\lambda / \beta \cos\theta$ where, λ= wavelength of X-rays, β = peak width of half maximum and θ=Bragg diffraction angle and the values are of about 16.9nm,15.9nm,13.2nm and 12.8nm for ZnO, Co-ZnO, In-ZnO and Co-In-ZnO respectively. It implies that the doping might inhibit the growth of ZnO.

Table.1: 2θ Values of ZnO, Co-Zno, In-ZnO and Co-In-ZnO

S. NO.	Plane (hkl)	ZnO (Standard) (2θ)	ZnO (2θ)	Co-ZnO (2θ)	In-ZnO (2θ)	Co-In-ZnO (2θ)
1	100	31.77	31.82	31.65	31.59	31.52
2	002	34.42	34.47	34.30	34.24	34.20
3	101	36.25	36.30	36.11	36.08	35.99
4	110	56.60	56.67	56.54	56.45	56.39
5	103	62.86	62.95	62.80	62.73	62.60
6	112	67.96	68.03	67.80	67.80	67.70

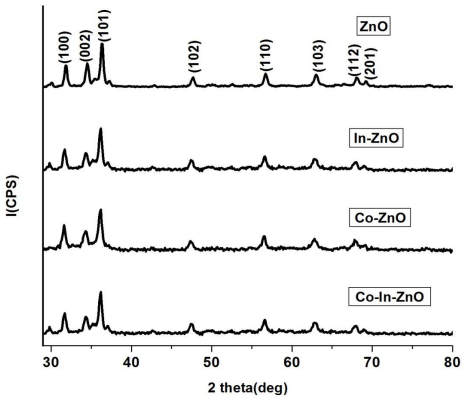

Figure 2: XRD Pattern of ZnO, Co-ZnO, In-ZnO and Co-In-ZnO

UV-vis DRS

UV-vis DRS was used to study the optical properties of ZnO, Co-ZnO, In-ZnO, and Co-In-ZnO nanoparticles and measured at room temperature in the wavelength range of 200-800nm as shown in Figure 3. The absorption edges of Co-ZnO, In-ZnO ,and Co-In-ZnO are slightly shifted to the visible region when compared to ZnO. Bandgaps of the ZnO, Co-ZnO, In-ZnO, and Co-In-ZnO nanoparticles determined from the Tauc plots are given in Figure 4. Band gap values are 3.13eV, 2.94eV, 3.12eV,and 2.82eV for ZnO, Co-ZnO, In-ZnO, and Co-In-ZnO respectively. The redshift of absorption edge corresponding to the bandgap narrowing could be attributed to the presence of cobalt and indium ions.

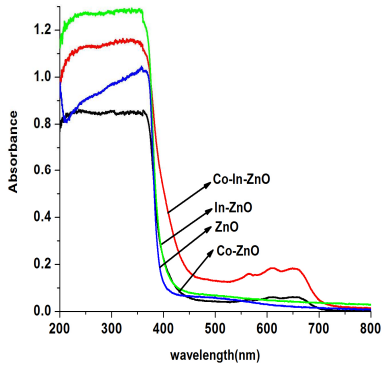

Figure 3: UV-vis Diffuse Reflectance Spectra of ZnO, Co-ZnO, In-ZnO and Co-In-ZnO

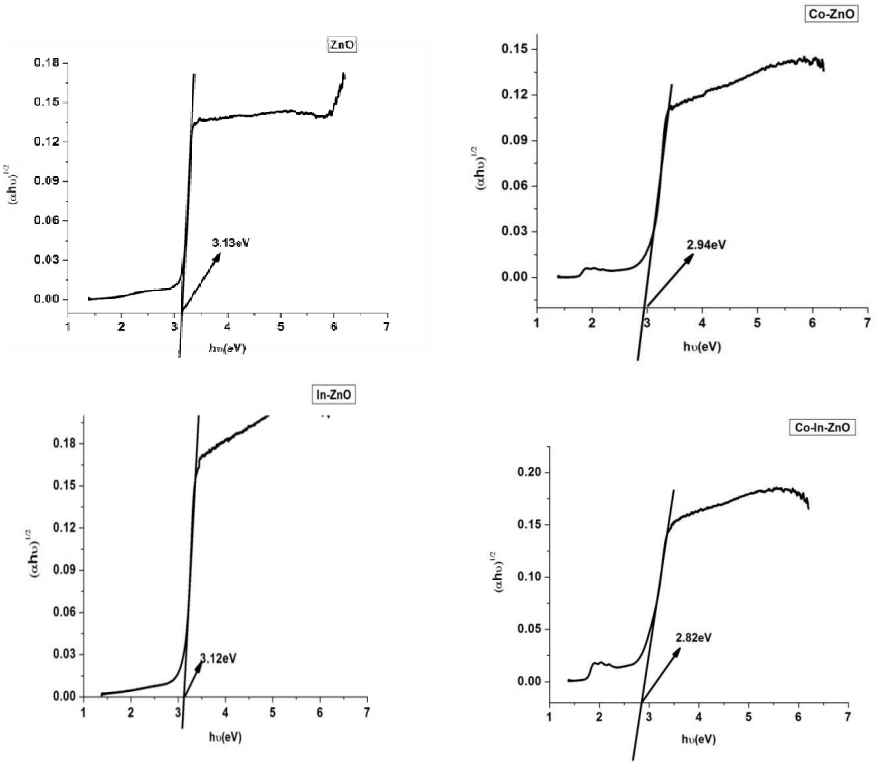

Figure 4: TAUC Plots of ZnO, Co-ZnO, In-ZnO ,and Co-In-ZnO

PL Spectra

The photoluminescence emission spectra of the ZnO, Co-ZnO, In-ZnO, and Co-In-ZnO were shown in Figure 5. The highest band intensity was observed for ZnO and lowest for Co-In-ZnO. The PL spectra can be used to examine the recombination of photoinduced electrons and holes. Therefore, lower the PL intensity for Co-In-ZnO reduces the recombination rate of photoinduced electrons and holes on the surface of ZnO. Thus, leading to enhanced photocatalytic activity [24, 25].

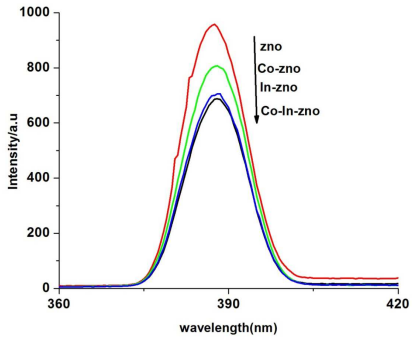

Figure 5: PL Spectra of ZnO, Co-ZnO, In-ZnO and Co-In-ZnO

SEM, TEM and EDX

The morphology of the samples was examined by SEM as shown in Figure 6. ZnO nanoparticles appear flower - like structure and Co-In-ZnO nanoparticles possess flake- like structures. So, these morphological changes induced by the addition of cobalt and indium ions. The morphology and particle size of the Co-In-ZnO were further characterized by

TEM. TEM images of Co-In-ZnO was shown in Figure 7. It reveals that, distribution of Co and In on the surface of ZnO. The average particle size of Co-In-ZnO is found to be around 20 nm. Energy dispersive spectra of ZnO, Co-ZnO, In-ZnO and Co-In-ZnO nanoparticles were displayed in Figure 8. EDX spectra of ZnO having only two elements, Zn and O indicate the purity of the ZnO sample and an additional Co and In elements exists in Co-In-ZnO nanoparticles.

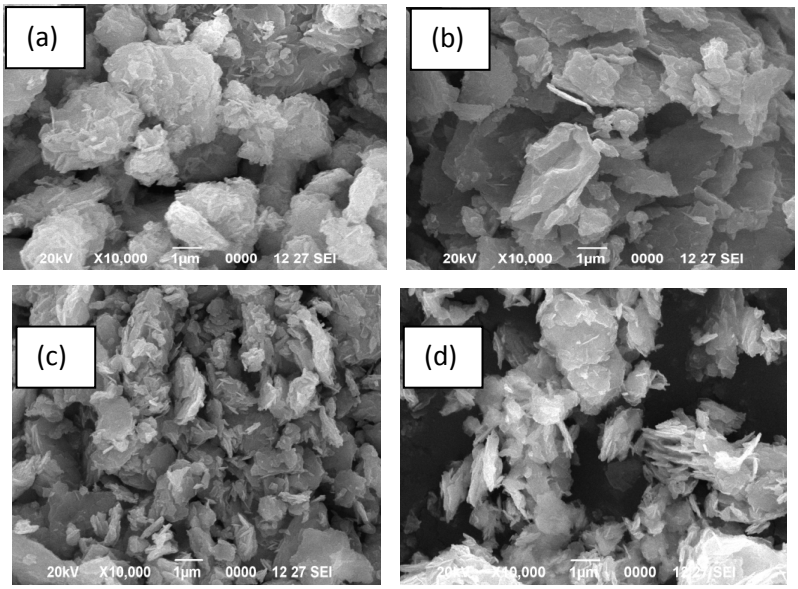

Figure 6: SEM Images of (a) ZnO (b) Co-ZnO (c) In-ZnO and (d) Co-In-ZnO

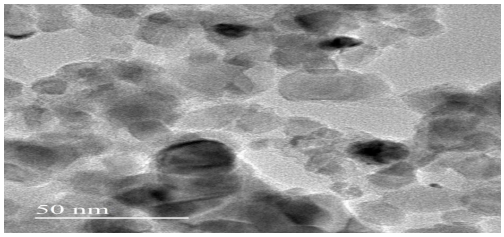

Figure 7: TEM image of Co-In-ZnO

Table.2. gives the ratio of Zn, Co, In and O elemental composition. The atomic percentages of the elements are obtained from the spectra and the doping of cobalt and indium was confirmed.

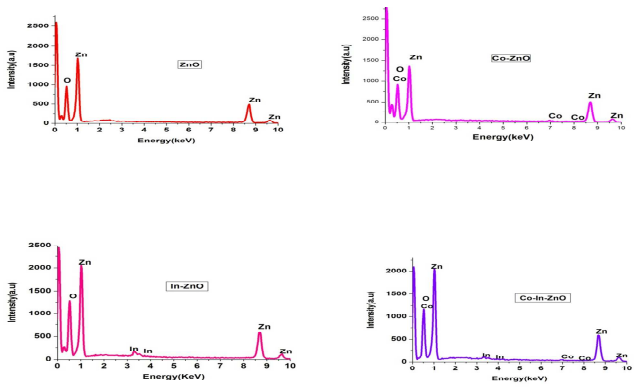

Figure 8: EDX Spectra of ZnO, Co-ZnO, In-ZnO and Co-In-ZnO

Table 2: EDX data of ZnO, Co-Zno, In-ZnO and Co-In-ZnO

Sample	Element	Atomic %	Weight %
ZnO	Zn	19.16	49.20
	O	80.84	50.80
Co-ZnO	Zn	19.57	49.46
	O	79.48	48.62
	Co	0.95	1.92
In-ZnO	Zn	18.17	47.74
	O	80.87	50.29
	In	0.96	1.97
Co-In-ZnO	Zn	18.12	47.41
	O	80.95	50.61
	Co	0.46	0.91
	In	0.47	1.07

B. E. T. Analysis

The surface area is important for determining the photocatalytic activity of Co-In-ZnO nanoparticles. The N_2-absorption -desorption isotherms of ZnO and Co-In-ZnO were displayed in Figure 9. The surface area ($S_{B.E.T.}$ (m^2/g)) and pore volume (cm^3/g) was calculated using B. E. T. Equation and the results are listed in Table.3. These isotherms are identified as hysteresis loops of type III. It is a characteristic of mesoporous (2-50 nm) materials according to the IUPAC classification [26]. The surface area and pore volume of the Co-In-ZnO are higher than that of ZnO. The increase in surface area is due to the presence of Co and In could significantly improve the photocatalytic activity.

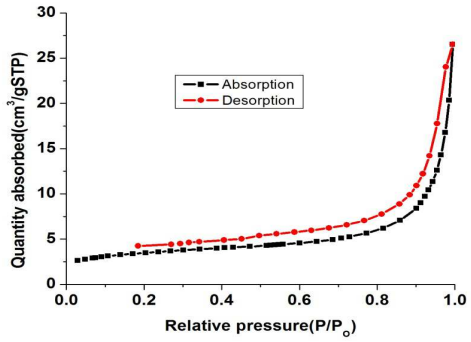

(a)

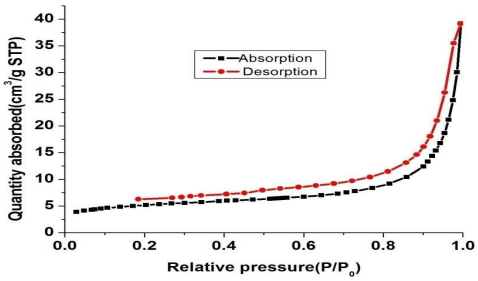

(b)

Figure 9: Nitrogen Adsorption-Desorption Isotherms of (a) ZnO and (b) Co-In-ZnO

Table 3: B. E. T Surface Area of Zn0 and Co-In-ZnO

Sample	$S_{B.E.T}$ (m^2/g)	Pore volume(cm^3/g)	Pore size(A^0)
ZnO	11.90	0.04104	137.96
Co-In-ZnO	17.56	0.06056	139.45

Photodegradation of MB

Photocatalytic activity of all samples was carried out with an initial concentration of 10 μM, a catalyst concentration of 0.5g/L, pH 10 and irradiation time of 180 min. Figure 10. Shows the MB degradation under visible light for various irradiation times (0 min, 30 min, 60 min, 90 min, 120 min, 150 min and 180 min) in the presence of Co-In-ZnO.

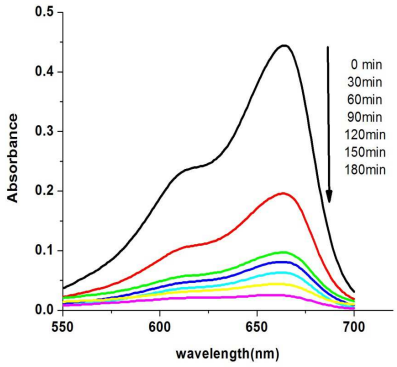

Figure 10: Absorption Changes of MB Photodegradation Process using Co-In-ZnO

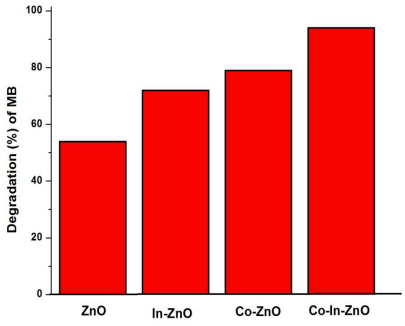

Figure 11: Effect of Catalyst (ZnO, Co-ZnO, In-ZnO, and Co-In-ZnO) On the Degradation of MB

The comparison of photodegradation percentage of MB over ZnO, Co-ZnO, In-ZnO, and Co-In-ZnO are shown in Figure 11. The results revealed that the doped ZnO showed higher photocatalytic activity than bare ZnO. The photocatalytic activity of Co-In-ZnO was found to be 94%. Therefore, doping of Co and In in ZnO significantly improves its catalytic activity.

A possible mechanism has also been proposed based on the previous reports [24, 27, and 28,] to explain the effects of Co and in dopants on the photocatalytic activity of ZnO. As shown in Figure 12. With the substitution of Co2+, a new impurity level is introduced closer to the conduction band of ZnO. The electrons can be excited from the valence band

to the conduction band or the impurity level under stimulated visible light irradiation. The existence of In3+ dopant within the crystal matrix or on the surface of ZnO can trap photogenerated electrons or holes and subsequently scavenged by the adsorbed oxygen and hydroxyl ions to generate superoxide radicals (O2._) and hydroxide radicals (OH) respectively. These processes effectively suppress the electron–-hole recombination. As it is well known that both superoxide and hydroxide radicals have strong oxidation power, which degrades the MB. Therefore, the photocatalytic activity of Co-In–ZnO is greatly improved.

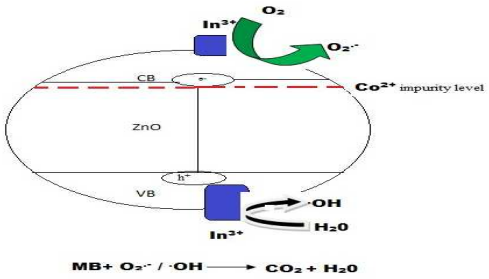

Figure 12: Schematic Diagram of Electron Transfer in Co-In-ZnO Under Visible Light Irradiation

Effect of pH

The effect of pH on the degradation of MB was examined in the pH range of 5 to 12 with an initial MB concentration of 10 µM and Co-In-ZnO concentration of 0.5 g/L. The results are depicted in Figure 13. The photodegradation of MB increases from pH value 5 to 10 and then it decreases with an increase in pH value 11. According to the point of zero charge (Pzc) of ZnO [pHPzc of ZnO = 9.3], the surface is positively charged in an acidic solution (pH< pHPzc) and negatively charged in alkaline solution (pH>pHPzc) [29, 30]. In a basic medium, the dye is strongly adsorbed on the photocatalyst surface owing to the strong electrostatic attraction between the dye molecule and catalyst and consequently the degradation is high. Since MB is a cationic dye, the electrostatic attraction between the dye molecule and catalyst is improved at pH10. However, further increasing the pH (above 10), which could reduce the hydroxyl ions due to breakage of hydroxyl ions at the catalyst surface. An acidic pH, the low photodegradation of MB is due to slight dissolution of ZnO [31].

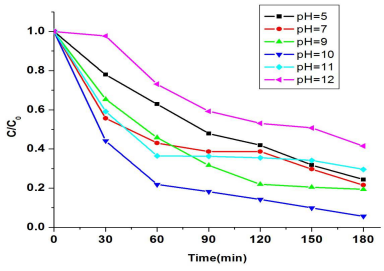

Figure 13: Effect of pH on the Degradation of MB

Effect of Initial MB Concentration

The effect of initial MB concentration on the photodegradation of MB was investigated in the presence of 0.5g/L of Co-In-ZnO at pH 10 was exhibited in Figure14. Photodegradation of MB decreases with increase in MB concentration from 10µM to 12µM. At high MB concentrations, more MB was adsorbed on the surface of the catalyst. Since the

availability of active sites remains the same at a fixed catalyst dosage. The dye molecules start acting as a filter for the incident light and result in a decrease in the rate of degradation of MB [32]. Hence, the optimum concentration of MB for better photodegradation was found to be 10µM.

Effect of Catalyst Dosage

The influence of catalyst dosage on the photodegradation of MB was studied by varying the Co-In-ZnO dosage from 0.25g/L to 1.0g/L and other reaction parameters were kept constant (MB concentration: 10 µM, pH=10) and the results are displayed in Figure 15. The photodegradation of MB increase with increase of Co-In-ZnO dosage from 0.25g/L to 0.5g/L and further increase in catalyst dosage leads to decrease in photodegradation. The observed increment in the photodegradation efficiency is due to the increase of the total active surface area and availability of the most active sites on the catalyst surface. The decrease in photodegradation efficiency above 0.5g/L may be due to the turbidity of the suspension and thus shielding the penetrating light [33, 34].

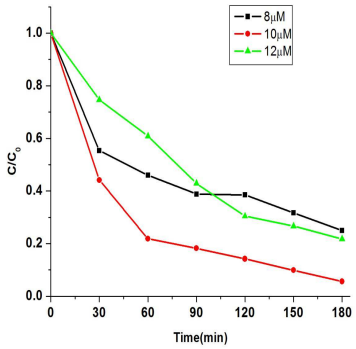

Figure 14: Effect of MB Concentration and its Photodegradation

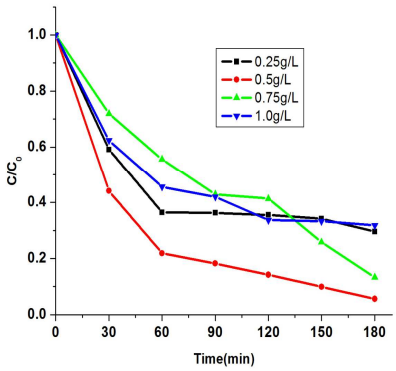

Figure 15: Effect of Catalyst Dosage on the Degradation of MB at pH 10

Photocatalyst Reuse and Stability

The ability to reuse Co-In-ZnO was evaluated by 4 successive cyclic experiments under the optimum reaction conditions (Co-In-ZnO = 0.5 g/L; MB = 10 µM and pH 10) and the results are presented in Figure 16. The photocatalyst obtained from the first run was filtered, washed several times with water and dried. Then, the recovered photocatalyst is used for the next run. The photodegradation percentage of MB for the four successive cycling of Co-In-ZnO were 94 %, 91%, 88 % and 85 % respectively. The photocatalytic activity of Co-In-ZnO is not diminished even after the fourth cycle

and the slight decrease in activity are attributed to the loss of photocatalyst during washing. In addition to that, there is no change in the XRD pattern of Co-In-ZnO [Figure 17] before and after the fourth photoreaction. The important crystalline phases are almost unchanged. These results revealed that the Co-In-ZnO is a stable photocatalyst for the degradation of dyes.

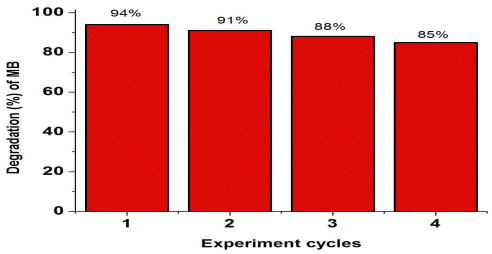

Figure 16: Reuse of Co-In-ZnO for the Photodegradation (%) of MB for Four Successive Cycles

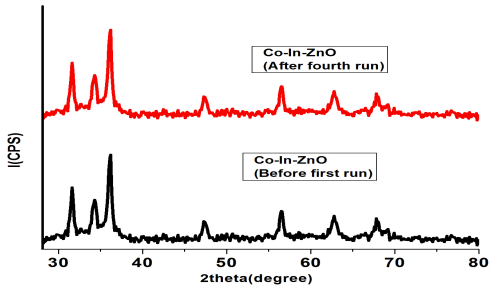

Figure 17: XRD Patterns of Co-In-ZnO before and after the Photoreaction

Antimicrobial Activity

The results of antimicrobial activity performed by ZnO Co-ZnO, In-ZnO, and Co-In-ZnO nanoparticles are shown in Table 4. It is seen from the Figure 18 (a) and (b) all the samples showed good antibacterial activity against Staphylococcus aureus and Escherichia coli.

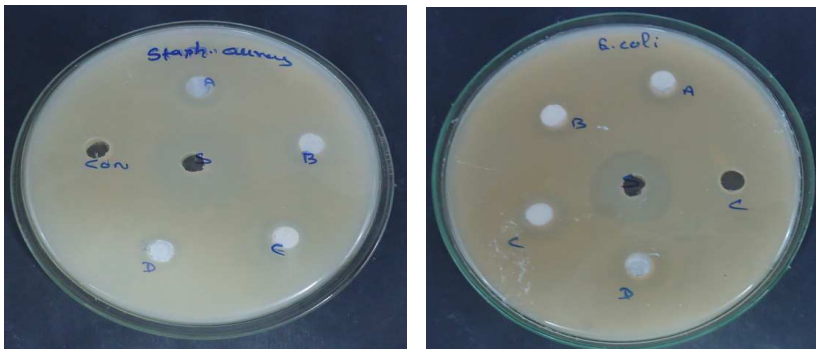

(a) **(b)**

Figure 18: Antibacterial Activity of Co-In-ZnO Against (a) *Staphylococcus Aureus* and (b) *Escherichia Coli*

Table 4: Antimicrobial Activity of ZnO, Co-ZnO, In-ZnO and Co-In-ZnO

Photocatalyst/ Standard	Diameter of Inhibition Zone (mm)		
	Bacterial Strains		Fungal Strain
	S. aureus	*E. coli*	*C. albicans*
ZnO (A)	12	13	15
Co-ZnO (B)	13	14	14
In-ZnO (C)	13	13	15
Co-In-ZnO (D)	15	15	16
Control (DMSO)	R	R	R
Standard (Amikacin)	19	19	-
Standard (ketokonazole)	–	–	16

Figure 19: Antifungal Activity of Co-In-ZnO against *Candida Albicans*

Antifungal activity of Co-In-ZnO gives the better results against Candida albicans [Figure 19]. The remarkable antimicrobial activity of ZnO, Co-ZnO, In-ZnO, and Co-In-ZnO are due to the generation of surface oxygen species which leads to the killing of the bacteria and fungi.

CONCLUSIONS

The Co-In-ZnO nanoparticles were prepared by co-precipitation method. The absorption edge of the Co-In-ZnO was extended to the visible light region. The photocatalytic degradation of MB proved that, Co-In-ZnO nanoparticles have a higher photocatalytic activity than ZnO, Co-ZnO,and In-ZnO. The photocatalytic efficiency was improved by the presence of the Cobalt and Indium dopants. The maximum percentage of MB degradation (94%) was achieved with a Co-In-ZnO dosage of 0.5g/L, initial MB concentration of 10µM, pH 10 and irradiation time of 180 min. Thus, Co-In-ZnO shows the potential application for the degradation of organic pollutants. All the samples showed better antibacterial activity against Staphylococcus aureus and Escherichia coli and antifungal activity against Candida albicans.

ACKNOWLEDGEMENT

The authors are thankful to the Management of N. M. S. S. V. N. College and Thiagarajar College for providing necessary laboratory facilities to carry out the work.

REFERENCES

1. *I. Fatimah, S. Wang, D. Wulandari, ZnO/montmorillonite for photocatalytic and photochemical degradation of methylene blue, Applied clay science, 53 (2011) 553-560.*
2. *B. Krishnakumar, M. Swaminathan, Influence of operational parameters on photocatalytic degradation of a genotoxic azo dye acid violet 7 in aqueous ZnO suspensions, Spectrochimica Acta Part A: Molecular and Biomolecular Spectroscopy, 81 (2011) 739-744.*
3. *S. K. Kansal, A. H. Ali, S. Kapoor, Photocatalytic decolorization of biebrich scarlet dye in aqueous phase using different nanophotocatalysts, Desalination, 259 (2010) 147-155.*
4. *M. Y. Guo, M. K. Fung F. Fang X. Y. Chen, A. M. C. Ng, A. B. Djurisic, W. K. Chan, ZnO and TiO_2 1D nanostructures for photocatalytic applications, Journal of alloys and compounds, 509 (2011) 1328-1332.*
5. *E. Pal, I. Dekany, Structural, optical and photoelectric properties of indium-doped zinc oxide nanoparticles prepared in dimethyl sulphoxide, Colloids and surfaces A: 318 (2008) 141-150.*
6. *C. Tian, W. Li, K. Pan, Q. Zhang, G. Tian, W Zhou, H. Fu, One pot synthesis of Ag nanoparticle modified ZnO microsphrers in ethylene glycol medium and their enhanced photocatalytic performance, Journal of solid state science 183 (2010) 2720-2725.*
7. *N. Morales-Flores, U. Pal, E. S. Mora, Photocatalytic behavior of ZnO and Pot-incorporated ZnO nanoparticles in phenol degradation, Applied catalysis A: General, 394 (2011) 269-275.*
8. *M. Bizarro, A. Sanchez-Arzate, I. Garduno-Wilches, J. C. Alonso, A. Ortiz, Synthesis and characterization of ZnO and ZnO: Al by spray pyrolysis with high photocatalytic properties, Catalysis today, 166 (2011) 129-134.*
9. *W. Xie, Y. Li, W. Sun, J. Huang, H. Xie, X. Zhao, Surface modification of ZnO with Ag improves its photocatalytic efficiency and photostabiliy, Journal of photochemistry and photobiologyA: Chemistry, 216 (2010) 149-155.*
10. *A. Nageswararao, B. Sivasankar, V. Sadasivan, Kinetic studies on the photocatalytic degradation of direct yellow 12 in the presence of ZnO catalyst, Journal of molecular catalysis A: Chemical, 306 (2009) 77-81.*
11. *N. V. Kaneva, D. T. Dimitrov, C. D. Dushkin, Effect of nickel doping on the photocatalytic activity of ZnO thin films under UV visible light, Applied surface science, 257 (2011) 8113-8120.*
12. *X. Li, Y. Cheng, S. Kang J. Mu, Preparation and enhanced visible light-driven catalytic activity of ZnO microrods sensitized by porphyrin heteroaggregate, Applied surface science, 256 (2010) 6705-6709.*
13. *R. Ullah, J. Dutta, Photocatalytic degradation of organic dyes with manganese-doped ZnO nanoparticles Journal of hazardous materials, 156 (2008) 194-200.*
14. *Y. Xu, H. Xu, H. Li, J. Xia, C. Liu, L. Liu, Enhanced photocatalytic activity of new Photocatalyst Ag/AgCl/ZnO,Journal of Alloys and Compounds,509(2011),3286-3289.*
15. *B. Donkova, D. Dimitrov, M. Kostadinov, E. Mitkova, D. Mehandjiev, Catalytic and photocatalytic activity of lightly doped catalysts M: ZnO (M=Cu,Mn),Materials Chemistry and Physics, 123 (2010) 563-568.*
16. *Y. Lu, Y. Lin, D. Wang, L. Wang, T. Xie, T. Jiang, A High Performance Cobalt-Doped ZnO Visible Light Photocatalyst and its Photogenerated charge Transfer Properties, Nano Research,4 (2011) 1144-1152.*
17. *H. Duan, H. He, L. Sun, S. Song, Z. Ye, Indium doped ZnO nanowires with infrequent growth orientation, rough surfaces and low density surface traps, Nano Scale Research Letters, 8 (2013) 493-502.*

18. *G. Xiao-Ming, F. Feng, W. Yu-Fei, Z. Li-Ping, L. Wen-Hong, Preparation of Co-$BiVO_4$ photocatalyst and its application in the photocatalytic oxidative thiophene, Journal of inorganic materials, 27 (2012) 1073-1078.*

19. *B. Zhou, X. Zhao, H. Liu, J. Qu, C. P. Huang, Synthesis of visible light sensitive M-$BiVO_4$ (M=Ag, Co, Ni) for the photocatalytic degradation of organic pollutants, Separation and purification technology,77 (2011) 275-282.*

20. *X. Yang, L. Xu, X. Yu, Y. Guo, One step preparation of Silver and Indium Oxide co-doped TiO_2 photocatalyst for the degradation of RhB, Catalysis Communication, 9 (2008) 1224-1229. [21] D. Sannino, V. Vaiano, O. Sacco, P. Ciambelli, Mathematical modeling of photocatalytic degradation of methylene blue under visible light irradiation, Journal of environmental chemical engineering, 1 (2013) 56-60.*

21. *P. Malathy, K. Vignesh, M. Rajarajan, A. Suganthi, Enhanced photocatalytic performance of transition metal doped Bi_2O_3 nanoparticles under visible light irradiation, Ceramic international, 40 (2014) 101-107.*

22. *M. G. Nair, M. Nirmala, K. Rekha, A. Anukaliani, Structural, Optical, Photo Catalytic and Antibacterial Activity of Zno and Co Doped ZnO Nanoparticles. Mater. Lett.65 (2011) 1797–1800.*

23. *S. Kuriakose, B. Satpati, S. Mohapatra, Enhanced photocatalytic activity of Co doped ZnO nanodisks and nanorods prepared by a facile wet chemical method, Phys. Chem. Chem. Phys., 16 (2014) 12741-12749.*

24. *X. Zou, X. Dong, L. Wang, H. Ma, X. Zhang, Preparation of Ni doped Zno-TiO_2 composite and their enhanced photocatalytic activity, Int. journal of photoenergy, 2014(2014)*

25. *K. Vignesh, R. Priyanga, M. Rajarajan, A. Suganthi, Photoreduction of Cr(VI) in water using Bi_2O_3-ZrO_2 nanocomposite under visible light irradiation, Materials science engineering B 178 (2013) 149-157.*

26. *K. Vignesh, M. Rajarajan, A. Suganthi, Visible light assisted photocatalytic performance of Ni and Th co-doped ZnO nanoparticles for the degradation of methylene blue dye Journal of Industrial and Engg. Chem.20 (2014) 3826-3833.*

27. *R. Arunadevi, A. Suganthi, B. Kavitha, P. Pandi Sudha, M. Rajarajan, Photocatalytic enhancing for tin oxide nanoparticles by co doping with nitrogen and bismuth, Desalination and Water Treatment, 78 (2017) 330-340.*

28. *C. Chen, J. Liu, P. Liu, B. Yu, Investigation of photocatalytic degradation of methyl orange by using nanosized ZnO catalysts, Advances in chemical engineering and science, 1 (2011) 9-14.*

29. *M. A. Chamjangali, S. Boroumand, Synthesis of flower like Ag-ZnO Nanostructure and its application in the photodegradation of methyl orange, Journal of Brazilian chemical society, 24(2013) 1329-1338.*

30. *E. Engenidou, K. Fytanos, I. Poulios, Semi-conductor sensitized photodegradation of dichloruos in water using $TiO_2$and ZnO as catalysts, App. Cat-B: Environ. 59 (2005) 81-89.*

31. *S. H. Borji, S. Nasseri, A. H. Mahvi, R. Nabizadeh, A. H. Javadi, Investigation of photocatalytic degradation of phenol by Fe(III)-doped $TiO_2$and T iO_2 nanoparticles, Journal of environmental health science and engineering 12 (2014) 101-110.*

32. *A. Ameta, R. Ameta, M. Ahuja, Photocatalytic degradation of MB over ferrictungstate, Sci. Revs. Chem. Common., 3 (2013) 172-180.*

33. *S. Selvarajan, P. Malathy, A Suganthi, M Rajarajan, Fabrication of mesoporous $BaTiO_3$/SnO_2 nanorods with highly enhanced photocatalytic degradation of organic pollutants, Journal of Industrial and Engineering Chemistry, 51 (2017) 201-213.*